International Journal of Architectural Heritage
Conservation, Analysis, and Restoration

ISSN: 1558-3058 (Print) 1558-3066 (Online) Journal homepage: http://www.tandfonline.com/loi/uarc20

Thin Folded Shell for the Renewal of Existing Wooden Roofs

Ezio Giuriani, Alessandra Marini & Marco Preti

To cite this article: Ezio Giuriani, Alessandra Marini & Marco Preti (2015): Thin Folded Shell for the Renewal of Existing Wooden Roofs, International Journal of Architectural Heritage, DOI: 10.1080/15583058.2015.1075626

To link to this article: http://dx.doi.org/10.1080/15583058.2015.1075626

Accepted author version posted online: 10 Aug 2015.
Published online: 10 Aug 2015.

Thin Folded Shell for the Renewal of Existing Wooden Roofs

Ezio Giuriani[1], Alessandra Marini[2], Marco Preti[3]

Abstract

In this paper, a technique for the renewal of historic building wooden roofs is presented. The solution can be used for the strengthening of existing wooden roofs against excessive lateral thrusts on the peripheral wall or for the recovery of the attics, as it allows removing the existing structural elements, such as possible wooden truss-works of no artistic value. With minor adaptations, the solution can be addressed to enhance the building seismic performance. The technique is minimally impairing on existing buildings and can be applied also in new constructions.

The technique is based on the construction of a thin folded shell, overlaying the existing pitches. Emphasis is given to lightweight folded shells, obtained by overlaying thin plywood panels on the existing roof rafters and planks, without modifying the overall architectural layout.

[1] Full Professor, Department of Civil Engineering, Architecture, Land and Environment, University of Brescia, Via Branze 43, 25123 Brescia, Italy.

[2] Associate Professor, Department of Engineering and Applied Science, University of Bergamo, Via Marconi 5, 24044 Dalmine, Bergamo, Italy.

[3] Assistant Professor, Department of Civil Engineering, Architecture, Land and Environment, University of Brescia, Via Branze 43, 25123 Brescia, Italy.

The technique conceptual design is discussed and a simplified analytical method is proposed, which allows clarifying the role of each structural component and can be adopted for the folded shell proportioning and design. The analytical results are validated against numerical results obtained with reference to some case studies. Ultimately, emphasis is given to the detailing, whose correct execution is mandatory for the success of the proposed structural intervention.

Keywords

Recovery of attics, strengthening or renewal technique, wooden roofs, historical building, folded roof shell, analytical model

1. Introduction

In this paper, a technique is proposed that can be usefully addressed for the recovery of historic building attics during restauration works. The technique conception and its first prototypal applications date back in the nineties (Fig.1, Giuriani 1997, Giuriani et al. 2002), and its effectiveness was confirmed by post-intervention monitoring. The solution is based on the construction of a thin and lightweight folded shell overlaying the existing roof pitch rafters and planks (Fig.2). Each pitch plane is transformed into a diaphragm, composed by the pitch joists, by perimeter chords and by a web panel overlaying the existing planks, which can be either made with wooden panels, a thin concrete slab or double crossed wooden planks (Fig. 3). For the solution to be effective, the pitch diaphragms must be properly connected to the perimeter walls.

The solution allows removing the existing structural elements supporting the roof from the intrados, such as the ridge beam and the possible existing wooden truss-works, thus it can be conveniently adopted when the attics recovery requires the clearing of the volume from existing wooden elements or partition walls. Obviously, removal of existing elements is viable when they are either severely degraded, or when their preservation is not mandatory. When clearing of the wooden trusses is required, the proposed solution is alternative and preferable to a possible and quite common intervention based on the adoption of a deep ridge beam, in substitution of the existing one, spanning the whole length of the attic floor, whose sagging should however be controlled to avoid introducing lateral displacements at the roof eaves.

Thanks to the control of the ridge sagging offered by the thin folded shell technique (chapter 2.3), the intervention can be conceived to strengthen the existing roof against the lateral thrust applied to the perimeter walls (Fig. 4). As a matter of fact, traditional hipped or saddle wooden roofs, composed by ridge beams and transverse joists, apply a lateral thrust to the crowning masonries, whose magnitude depends on the roof pitch angle, on the bearing loads, and on the flexibility of the roof structural elements. If the ridge beam is markedly deformable and the rafters are hinged to the perimeter masonries, the bending deformation of the ridge beam induces a lateral displacement at the eaves supports, which results in an overturning action applied to the perimeter walls (Fig. 4a; Griffith et al., 2003; Giuriani and Marini 2008b); the resulting perimeter wall drift can be as large as to cause damage of the masonry walls (Fig. 4b).

The first prototypal application of the thin folded shell solution was inspired by a real case intervention, whose main aim consisted in protecting the “Loggetta Veneziana“ of the San

Faustino Palace (Brescia, Fig.1b) against excessive out of plane deformations induced by the roof lateral thrust. Other applications followed over the years (see chapter 4). With some necessary adaptations, the roof folded shell technique was as well effectively addressed to enhance the seismic performance of some existing buildings (Giuriani and Marini, 2008a, Giuriani and Marini, 2008), such as a few churches damaged by the recent earthquakes of Salò (2004) and Emilia (2012).

Folded roof diaphragms are designed with reference to both resistance and deformation criteria, in order to support the roof dead load and the snow live load, and to limit the deformation and wall drift within acceptable values.

The folded roof shell technique can be preferably applied to building having regular geometry, namely: gable, pent, hipped, and hipped-gable roofs, characterized by either single or multiple bay roofs. For the sake of clarity, in the present work, reference is made to gable roofs only (Fig. 2).

The paper focuses on the structural behavior and on the conceptual design of the folded roof diaphragms with respect to vertical loads and aims at clarifying the static role and relevance of each structural member, the role of the inner web panel and that of the steel ribs and chords, as well as the importance of the connections between the diaphragms and the masonry walls. A simplified analytical approach, based on the limit analysis, is introduced to facilitate the understanding of the structural behavior and is addressed to guide the correct design of the whole folded roof diaphragms and the proportioning of each structural element. In the paper, a case study is commented to illustrate the proportioning criteria, and to compare analytical and

numerical results. Ultimately, the importance of the structural detailing is discussed by introducing some real case studies.

2. Design criteria and proportioning of folded roof shell against vertical loads

In the design the pitch planes are transformed into continuous diaphragms. To this end, different techniques can be adopted, which are commonly used for the flexural strengthening of wooden floors. In the particular case of roof diaphragms, techniques avoiding significant increase in the structural weight, and therefore in the seismic action, are usually preferred, especially for those buildings located in seismic prone areas. Accordingly, roof diaphragms should be preferably obtained by overlaying light plywood panels, connected to each other by means of nailed steel plates (Fig. 5a; Giuriani et al., 2002; Peralta et. al., 2004). Alternatively, the pitch diaphragms can be arranged by superimposing two layers of inclined wooden planks (Giuriani et al., 2014; Fig. 5b). The two layers of orthogonal wooden planks (as proposed in Benedetti et. Al., 1981; Fig. 5c), can be excessively deformable and thus unsuitable for this kind of intervention.

The solution of the thin ordinary concrete slab, which is commonly adopted for the flexural strengthening of wooden floors (Piazza and Turrini, 1983; Giuriani and Frangipane, 1993; Gelfi and Ronca, 1993; Fig. 5d) can be as well applied for the strengthening of wooden roofs. However, given the significant increase in the dead loads, this solution should be discarded in the case of delicate restoration works in highly seismic prone zone. The use of high performance

concrete, that allows reducing the slab thickness, can be regarded as an improvement of the traditional concrete slab technique (Meda and Riva, 2001; Fig. 5e).

Performance based design approach

The design of the folded roof shell is usually conceived to comply with the resistance criterion, i.e. every single structural component is proportioned to withstand a specific internal action in order to allow the transferring the vertical loads to the head gable walls (Giuriani 1997). Beside the resistance approach, the control of the structure deformation may be necessary to limit the in-plane deflection of the pitch diaphragms and thus the drift of the perimeter walls.

The simplified approach here proposed aims at determining the structure carrying capacity and at controlling the deformability. The conceived approach allows clarifying the behaviour of the folded roof diaphragms and identifying the static role of each structural component to finalise its proportioning. In the case of stiff structures, i.e. concrete roof diaphragms, deformations are usually negligible and the structure proportioning is governed by the resistance criterion. On the other hand, in the case of deformable structures, i.e. double layer plank structures (Fig. 4c), the proportioning could be governed by the control of the maximum deformations.

It is worth noting, however, that the simplified approach is not meant as an alternative to other more sophisticated approaches, such as the classical folded plate theory (Bruhn, 1973; Timoshenko, 1989) and the Finite Element method, which are needed when modelling irregular and complex buildings. Conversely, the proposed approach provides approximated solutions, which can be used as reference solutions to verify the results given by sophisticated approaches.

Ultimately, for the folded roof shell design, beside the whole structure behaviour, particular attention has to be paid to the structure detailing and the mutual connections between the single components, which play a fundamental role.

In the following discussion, reference is made to symmetrical gable folded roof shell only; minor adjustments are required for the method to be adopted for the analyses of hipped roofs of unsymmetrical geometry (Giuriani et al., 2002). Diaphragms made of wooden elements are considered; the approach can be easily extended to those solutions adopting either steel plates or thin concrete diaphragms.

2.1 Thin folded shell conceptual design

Each gable roof pitch is transformed into a shear resisting diaphragm, which transfers the pitch rafter lateral thrusts to the head gable walls (Giuriani 1997).

The main structural elements composing the thin folded roof shell are: the pitch rafters sustaining the "web"-panel (*1*), the ridge and eave chords *($c_{11,}$ c_{13})*, the head gable chords *(c_{12})*, and the head gables (*2*) (Fig.5a).

The pitch diaphragms are assumed to behave like chord and panel structures, in which the ridge and eave chords withstand in-plane bending and the pitch panel resists shear forces (Bruhn, 1973). In the elastic field, this hypothesis is accurate anytime the thickness of the web panel is evanescent with respect to the eave chord cross sections. In case of plywood web panels and steel chord structures, the web thickness is usually not evanescent. However, the presence of deformable nail connections, significantly reduces the global stiffness of the diaphragms. The

nail connected web panels can be regarded as equivalent to an ideally homogeneous panel of reduced mechanical properties. This way, the rate of the chord cross section over the ideal web panel cross section significantly increases, thus justifying the assumption of the chord and panel structure model. The chord and panel behavior is thus adopted in the elastic field as it simplifies the solution in a conservative way. Furthermore, for this kind of structure, the assumption of chord and panel structure behavior provides a reliable estimate of the response when the structure approaches collapse. Approaching the collapse mechanism, if a constant nail spacing is adopted, the plasticity of the nailed connections results in a constant uniform shear flow. The deformation induced by bending are negligible provided that the chords do not yield at the mid span. In this case, no significant curvature occurs into the pitch diaphragm. This way the nail connections do not appreciably contribute to bending resistance. By neglecting their contribution the solution is conservative for the chords. The accuracy of this approximation is confirmed by the numerical analyses (cap. 3), in which analytical and numerical solutions show negligible differences.

The proposed design method is based on the following simplified assumption: a) the diaphragms behave as membrane and have negligible torsion stiffness; b) the wooden panels are over-resistant; c) the deformation capacity is lumped in the nailed connections, which are characterized by large ductility (Humbert et al. 2014); d) the eave chords under traction are assumed to behave elastically; the buckling collapse of the compressed ridge chord is prevented by assembling two steel plates, which behave like angle type steel profile.

The design of the main structural elements composing the folded roof diaphragms is based on the hypothesis that the head gables (*2* in Fig. 3) behave like in-plane rigid diaphragms. The pitch rafter-to-wall connection is modelled as hinged; whereas, depending on the actual configuration, the rafter-to-rafter constraints along the roof ridge can be assumed as either hinged or clumped. The perimeter wall footing is connected to the lower masonries. In this scenario, the unit width frame (*A* in Fig. 6a) constrains are those shown in Figure 6b.

In order to evaluate the internal forces in the folded roof diaphragm, a two-step approach is addressed (Fig. 6), namely: (i) vertical and horizontal additional auxiliary constraints are introduced along the roof ridge line (Fig. 6b); (ii) auxiliary constraints are removed and their reaction forces are backed out (Fig. 6c).

In the first step, unit frame (*A*), with auxiliary vertical and horizontal constraints on the roof ridge, undergoing vertical loads p_1, behaves like a frame, whose internal forces can be easily evaluated. Roof rafters are subjected to axial force and bending moment, whereas the perimeter walls undergo vertical compression, n_a. Given the auxiliary constraints, no lateral displacement occurs at the eaves level (nodes 2 and 4, Fig. 6b).

In the second step, the auxiliary ridge constraint reaction forces (r_{1y} and r_{1z}) are cancelled by applying forces of equal intensity and opposite sign to the folded roof diaphragms. It is worth noting that only the vertical reaction must be cancelled ($f_{1z} = - r_{1z}$), as the symmetry of the problem entails zero horizontal forces ($r_{1y} = 0$).

Depending on the rafter mutual constraint at node 3, the vertical load applied to the folded roof shell along the ridge axis is equal to:

$$\begin{cases} f_{1Z} = p_1 l_{12} & \text{(a)} \\ f_{1Z} = \frac{5}{4} p_1 l_{12} & \text{(b)} \end{cases}$$

Case of hinge constraint at the ridge support

Case of rafter continuity at the ridge support (1)

where l_{12} is the pitch diaphragm width; and $p_1=g+q\cos\alpha$ (where: g is the dead load, q is the service load, α is the pitch angle).

The vertical load f_{1z} is decomposed along the pitch planes, as shown in Figure 7a, thus the load applied to each pitch diaphragm is equal to:

$$f_1 = \frac{f_{1z}}{2\sin\alpha} \qquad (2)$$

Each pitch diaphragm can be modelled as a deep beam, simply supported on the head walls, undergoing in plane uniform load per unit length f_1. The maximum bending moment, along the x axis, at the diaphragm mid span is equal to $M_X=f_1 L_X^2/8$, and the maximum shear at the head gable supports is $V_X=f_1 L_X/2$ (Fig.7a), being L_x the pitch diaphragm span.

Given the already discussed assumption, the bending moment is resisted by the external chords, whereas the shear force is resisted by the web panel. Therefore, the maximum bending moment is balanced by two axial forces F_{11} and F_{13} acting on the ridge and eave chords, respectively (Fig. 7a):

$$F_{l1}=-F_{l3}=\frac{M_X}{l_{12}} \quad (3)$$

whereas the maximum shear force at the supports entails a shear flow q_1, which is resisted by the panel:

$$q_1=\frac{V_X}{l_{12}} \quad (4)$$

Concerning the proportioning of the gable roof pitch diaphragms, ridge and eave chord cross sections are proportioned to resist the axial forces $2F_{l1}$ and F_{l3}, respectively (eq.3).

The pitch panel thickness, the pitch panel mutual connections, as well as the connection of the panels to the head gables are proportioned to resist the maximum shear flow q_1 (eq.4, Fig.7a). When plywood panel are adopted, the spacing of the nailed connections between adjoining panels can be increased along the x-axis, as the shear flow decreases approaching the diaphragm mid-span. For the same reason, the spacing of the nail connecting the web panel and the longitudinal ridge and eave chords can be as well increased.

Web panel-to-rafter connections

As for the roof diaphragm behavior, some modelling assumptions require further explanation. In the model the auxiliary constraints are assumed as uniformly distributed along the ridge line, and the ridge load per unit length f_{lz} (f_{lz}=-r_{lz}) is transferred to both diaphragms as an action per unit length f_l (eq.2, as shown in Fig.7a). In the real structure the vertical reaction applied to the

folded roof shell is lumped at the rafters end section, thus $R_r=r_{1z}\, i=-f_{1z}\, i$ (Fig. 7b). The reaction force R_r is balanced by the rafter axial force N_r, thus it yields: $N_r=f_1 i$. The axial force N_r is transferred to the web panel *1* by the dowel connectors *d* between the rafters and the pitch diaphragms (Fig.6b,c); each dowel connector *d* transfers a point load equal to $V_d= f_1\, i/n_d = N_r/n_d$ (where n_d is the number of connectors) (Fig.7d).

Pitch diaphragm-to-lateral wall connections. In the case of folded roof shell resisting the seismic actions, the connections between the diaphragm *1* and the top lateral walls *3* is fundamental as to avoid the possible perimeter wall detachment and overturning and to trigger a box structure behaviour of the whole construction (Giuriani and Marini, 2004 and 2008). To this end, dowel connections can be conveniently adopted (d_m in Fig. 7e; Gattesco and Del Piccolo, 1998; Felicetti et al., 1997).

Conversely, when resistance against the sole gravitational loads is required, dowels d_m are usually not mandatory because no shear forces are transferred between the roof and the peripheral walls. Dowels d_m would be necessary in the case of gravitational loads only if the rafter restraint behaved like an inclined sliding support, in which case the dowel connection would avoid the wall thrust induced by the inclined reaction force, which in turn would induce the bending of the wall (Giuriani 2012). Regardless the particular restrain, the adoption of dowels d_m is suggested anyway in order to guarantee a minimum box structural behaviour.

Finally, nailed connections must be adopted to transfer the longitudinal shear flow between diaphragm *1* and eaves chord c_{13} (Fig. 7e).

Head gable-to-diaphragm and wall-to-diaphragm connections

The role of the rigid head diaphragm supporting the roof folded shell (*2* in Fig. 3) is usually played by the head masonry wall or by the head wooden truss-works. The head wall has to be engineered with appropriate devices in order to resist to the shear flow q_1 (eq. 4). Particular attention must be paid to the detailing of the head wall system. The simplest solution is shown in Fig. 8a, where the shear flow q_1 is directly transmitted to the upper part of the wall by means of the dowel connectors d_m: the masonry develops two inclined strut, whose thrust is confined by the horizontal steel ties *T,* suitably anchored to the wall edges (Giuriani 2012). Ties *T* can be accommodated either within holes drilled in the masonry wall (Fig. 8a') or alongside the wall lateral surfaces (Fig. 8a''). Furthermore, in order to increase the efficiency of the connection between the wooden pitch diaphragm and the head wall crowning masonries, the diaphragm is reinforced at the supports by additional extrados steel ribs (c_{12} in Fig. 8a'), which are nailed to the wooden elements (*1*) and fastened to the walls by means of steel dowels (d_m). Finally, in order to withstand the concentrated loads transferred by the dowels, the upper edge of the head wall should be strengthened; to this end a suitable technique is represented by the adoption of a thin 2-3cm lime plaster slab reinforced with a few fiber mesh layers.

As an alternative solution, in order to resist the shear flow q_1, a "structural saddle" (Fig. 8b) can be engineered on top of the head walls by appropriately arranging the steel ribs c_{12}.

Particular attention must be paid to the ridge joint. This joint must resist the rib tensile action *N* caused by the shear flow and the vertical concentrated reactions *R*:

$$N=q_1 l_{12}$$

$$R= 2N \sin \alpha$$

Figure 8c represents a possible design mistake that might come across when no ties are adopted and the possible gap between steel ribs and the upper wall is neither filled nor engineered to sustain the vertical component R of the traction forces N of the rafters converging at the ridge (Fig.8b,c).

The solution in Fig. 8d illustrates the arrangements of the head inclined wooden beams, which can be directly nailed to the wooden diaphragm, when the ridge mid-support is available; the lateral thrust of the beams can be confined by the steel tie (*T*). Finally, in Figure 8e the wooden beams and the ties (*T*) must be conceived as to obtain a truss work-like structure. In all cases, the connections between the wooden pitch diaphragm *1* and the head wall has to be arranged as in case *a*.

2.2 Additional stay-structure

The assemblage of the diaphragms by means of plywood panels might be impracticable for long spanned roofs (over 30-40m length), as an unrealistic number of nail mutual connections of the web panels would be required to withstand the large shear flow. For the plywood sheathing solution to be still feasible, a supplementary resisting and stiffening system, providing additional shear resistance, may be conveniently adopted. In the following, the use of a steel plate stay-structure, overlaying the wooden sheathing structure, is proposed (Fig. 9). An application of this solution to a monumental building is illustrated in Figure 1b.

Within the elastic field of response, the relative stiffness of the two systems in parallel will determine the distribution of stresses among them; but considering the system ultimate capacity, by assuming the perfect ductility of the steel flanges under traction forces and of both the nail and the stud connection at collapse and assuming the plywood panels be over-resistant, the roof pitch ultimate shear resistance can be easily evaluated by adding the shear resistance of the stay structure and that of the pitch diaphragm web (Fig. 10).

Two types of failure of the strengthened folded roof shell might be expected: shear failure, usually occurring at the head gable support, and flexural failure at mid span. Hence, the ultimate load per unit length f_{lu} is the minimum load triggering either a shear or bending failure of the pitch diaphragm, alternatively.

The bending resistance corresponds to the yielding of the eave or ridge chord (i.e. $F_{l3} = A_{13}f_{yd}$), thus the load triggering the bending failure, $f_{u,B}$, is equal to:

$$f_{u,B} = \frac{8A_{13}f_{yd}l_{12}}{L_x^2} \tag{5}$$

It is worth noting that the adoption of the supplementary stay structure does not modify the bending capacity of the pitch diaphragm, which is governed by the chord resistance at mid span. The compression force along the ridge, equilibrating the horizontal component of the stay axial force at the support (detail A, Fig. 9), is transferred through a welded connection fixing the stay to the longitudinal ridge chord. Each stay element along the span has to be as well welded to the

eaves chord to transmit the longitudinal component of the stay axial force. Furthermore, the transverse component of the axial traction force of each stay is transferred to elements *a*, which are nailed to the pitch web panel (detail B, Fig. 9); thus element *a* (detail C) spread the concentrated load transferred by the stay structure to the pitch diaphragm.

Note that both the vertical component of the stay traction force $V_{st,j} = F_{st,j}\ sen\ \alpha_j$ and the additional shear flow $\Delta q\ l_{12} = (\Delta q/\Delta x)\Delta x\ l_{12}$, are equilibrated by the ridge force $f_1\Delta x$ (detail C in Fig.9), being α_i the stay inclination and Δx the distance between the stays along the eave chord.

By assuming perfect plasticity of the materials, the shear resistance (V_u) is provided by both the web panel ($V_{u,wp}$) and the stay structure ($V_{u,st}$) (Figure 10), thus:

$$V_u = V_{u,wp} + V_{u,st} \tag{6}$$

where the shear resistance of the diaphragm web $V_{u,wp}$ is equal to the resistance of the nailed connections, assuming the web plywood panel as being over resistant, and the maximum shear resistance at the pitch diaphragm support provided by the stay structure is equal to:

$$V_{u,st} = \sum_{i=1}^{N_{st}} f_{yd} A_{st} \text{sen}\alpha_i \tag{8}$$

where N_{st} is the number of steel stays. The shear resistance contribution provided by each stay in the plane of the diaphragm is given by the y' component of the traction force in the stay. This

way, the shear resistance of the stay structure $V_{u,st}$ varies saw-tooth wise along the span, as shown in Figure 10a. The web panel resistance $V_{u,wp}$ is constant according to the assumption of constant spacing of the nails connecting neighboring panels. Thus an accurate check that the shear force distribution V_{sd} be entirely contained within the shear resistance domain ($V_u = V_{u,st} + V_{u,wp}$) along the x axis is necessary. Note that if the shear force V_{sd} is smaller than the shear resistance of the web panel $V_{u,wp}$, then no stays are required. Figure 10a shows an example of shear failure at the supports, where the shear force V_{sA} is maximum and equal to the resistance V_u (point A). Figure 10b illustrates a situation where shear failure occurs along the span (point B), where the shear force V_{sB} is greater than the shear resistance Vu. The latter stay layout, which does not allow entirely exploiting the shear resistance, should be improved by introducing additional stays. Provided that the shear failure is first reached at the support, the ultimate load is equal to:

$$f_{u,V} = \frac{2V_u}{L_x} \tag{9}$$

Hence, the folded roof shell ultimate load (f_u) is the minimum load triggering the shear or flexural resistance, alternatively:

$$f_u = \min\left\{f_{u,B}; f_{u,V}\right\} \tag{10}$$

Note that, for practical application, the bending resistance is rarely overcome, whereas the failure is usually governed by the folded roof shell shear capacity.

2.3 Simplified evaluation of the structure deformability

In the following a simplified method for the evaluation of the folded roof shell elastic horizontal displacements along the eaves line is introduced. The maximum horizontal displacement at the mid span yields the maximum drift of the masonry wall. It is worth noting that, depending on the structure stiffness, the deformability control might be an issue for folded roof shell made of plywood panels and steel chords, whereas it is almost negligible in the case of stiffer concrete overlays.

The pitch diaphragm is modelled as a simply supported beam undergoing a uniform load per unit length f_1. The maximum in-plane displacement of the pitch diaphragm at the mid span can be evaluated by adding the contribution of the in plane bending deflection and shear deformability and neglecting deformations induced by the diffusion of concentrated loads. Accordingly, it is possible to integrate the second derivative of the elastic line, in which both bending and shear deformability are taken into account:

$$y''(x) = -\frac{M(x)}{E_w^* J_{id}} - \frac{\chi}{G_w^* A_w} \cdot \frac{d^2 M(x)}{dx^2} - \Delta y'' \tag{11}$$

where E_w^* and G_w^* are the Young and shear moduli of the plywood panel, which account for the shear deformability of the nails connecting neighboring panels (see next paragraph); J_{id} is the

second moment of area of the ideal transformed cross section, evaluated by introducing the coefficient $n^{*}=E_s/E_w^{*}$; A_w is the web panel cross section; and $\Delta y''$ is the incremental curvature entailed by the slip along the horizontal connections between web panels and ridge and eave chords (see next paragraph).

The maximum in-plane displacement at the pitch diaphragm mid span ($x = L_x/2$) is equal to:

$$y_{max}=\frac{5}{384}\frac{f_1 L_x^4}{E_w^{*} J_{id}}+\frac{\chi}{8G_w^{*}A_w}f_1 L_x^2+\Delta y \qquad (12)$$

where Δy is the incremental deflection due to $\Delta y''$.

Note that in case of thin concrete folded roof diaphragm, the Young and shear modulus of concrete should be used instead and $\Delta y''=\Delta y=0$ in equations 11 and 12.

Unlike the single isolated pitch diaphragm, the two pitch diaphragms composing the folded one cannot freely deform in their plane. Continuity of the folded roof along the ridge line is guaranteed by assuming negligible torsion stiffness of the folded roof and by enforcing a pure membrane behavior. This way, single pitch diaphragm in-plane deformation caused by in-plane bending induces the whole folded roof shell cross section deformation. As a result of the pitch diaphragm mutual connection along the ridge line, and because of the connection to the masonry wall along the eaves line, the folded roof shell can only sag vertically along the ridge and slide horizontally along the eaves. By referring to the Kinematic shown in Figure 11, an estimate of the vertical sag along the ridge line and horizontal slide at the eave supports can be derived. By

assuming that the pitch diaphragm width does not vary, vertical (w_{max}) and horizontal (η_{max}) displacements are calculated based on the maximum in-plane deflection y_{max} of the pitch diaphragm. In the small displacement field, it yields:

$$w_{max} = \frac{y_{max}}{\text{sen}\alpha} \qquad \eta_{max} = \frac{y_{max}}{\cos\alpha} \tag{13}$$

therefore:

$$\eta_{max} = \tan\alpha \, w_{max} \tag{14}$$

For roof sloping ranging between α=18÷24°, the estimated lateral displacement is equal to $0.32 \div 0.44 \, w_{max}$.

Shear deformability of wooden diaphragm induced by the web panel connections

In the case of plywood folded roof shells, depending on the panel arrangement, the deformability of the entire structure is strongly affected by the shear slips of the nail connections: a) slips occurring along neighboring panels stripe (alignment *a* in Fig. 12a), slips along the horizontal joints at the web panel mid height (alignment *b* in Fig. 12a) and along the joints of the eave and ridge chords and the web panel (alignment *c* and *c'* in Fig. 12a).

- In order to account, in a simple fashion, for the reduction of the bending and shear stiffness caused by the panel mutual connections (alignment *a* in Fig. 12a), the mechanical properties of the plywood panel can be modified and equivalent Young (E_w^*) and shear (G_w^*) modulus can be introduced.

The equivalent shear modulus (G_w^*) can be evaluated by reference to the panel stripe pertaining to each nail (having width Δx_n) illustrated in Figure 12b. The total shear displacement s_{tot} between adjacent plywood panels is given by the addition of the nail slip s_n and the elastic wood panel shear deformation γ_w:

$$s_{tot} = 2s_n + \gamma_w l_p \qquad (15)$$

being l_p the panel width.

The connection shear slip s_n is given by the elastic relationship:

$$s_n = V_n / k_n \qquad (16)$$

where k_n is the single nail shear stiffness, which can be obtained either experimentally, or by reference to formulations provided by the literature (i.e. Eurocode 5, 2005, Giuriani et al., 2001).

The ideal shear deformation γ_w^* is:

$$\gamma_w^* = \frac{s_{tot}}{l_p} \qquad (17)$$

Given that the shear stress and distortion are respectively equal to: $\tau_w = V_n / A_{wn}$ and $\gamma_w = V_n / \left(A_{wn} G_w \right)$, by substituting eq.15 and 16 in eq.17, the ideal shear modulus $G_w^* = \tau_w / \gamma_w^*$ becomes as follows:

$$G_w^* = \frac{k_n l_p}{2A_{wn} + \frac{k_n l_p}{G_w}} \quad (18)$$

where $A_{wn} = \Delta x_n t$ is the panel stripe cross section area, Δx_n is the nail spacing and *t* is the panel thickness.

The equivalent Young modulus (E_w^*) is evaluated by considering the unit panel stripe in Figure 12c. The total displacement caused by the tensile force (F_n) across the panel stripe is equal to:

$$2s_n + \varepsilon_w l_p = \varepsilon_w^* l_p = \frac{F_n}{A_w E_w^*} l_p \quad (19)$$

being ε_w and ε_w^* the plywood panel and the equivalent panel axial strains, respectively.

By rearranging eq.16, the equivalent Young modulus (E_w^*) can be obtained:

$$E_w^* = \frac{k_n l_p}{2A_{wn} + \frac{k_n l_p}{E_w}} \quad (20)$$

Note that the plywood deformability plays a significant role in the appraisal of the equivalent panel characteristics. By neglecting the panel deformability, i.e. by setting E_w and G_w equal to infinity in eq.18 and eq.20, and by assuming ordinary values of the geometric and mechanic properties (l_p = 1200 mm, A_{wn} = 50 mm·27.5mm, E_w= 5000 MPa, G_w= 2500 MPa, k_n = 2700 N/mm), a 25% overestimate of the ideal Young modulus E_w^* and a 50% overestimate of the shear modulus G_w^* are obtained.

- In order to account for the incremental deflection caused by the nail connection slip at the panel mid height $s_{n,b}$ (double nail connection along alignment *b* in Fig. 12a, $s_{n,b}=2s_n$) and at the eave and ridge chord level $s_{n,c}$ and $s_{n,c'}$ (single nailed connections along alignment *c*, $s_{n,c}=s_n$, and *c'*, $s_{n,c'}=s_n$, in Fig. 12a), reference is made to the theory presented in Gelfi and Giuriani, 2009. The slips occurring along these horizontal alignments cause an incremental rotation at the supports (Fig. 12d), which is equal to:

$$\Delta\varphi=\frac{s_{n,b}+s_{n,c}+s_{n,c'}}{H}$$

This incremental rotation entails an additional deflection at the diaphragm mid span. With reference to the case of the simply supported beam undergoing uniformly distributed load, the additional deflection is equal to:

$$\Delta y_{max}=\frac{\Delta\varphi L_x}{3.2}$$

This contribution must be added to the maximum deflection calculated in eq. 12. Thus, in the case of plywood pitch diaphragms with panels arranged as in Figure 12a, the maximum deflection can be calculated as follows:

$$y_{max} = \frac{5}{384}\frac{f_1 L_x^4}{E_w^* J_{id}} + \frac{\chi}{8 G_w^* A_w} f_1 L_x^2 + \frac{s_{n,b} + s_{n,c} + s_{n,c'}}{3.2\,H} L_x \qquad (12')$$

3. Case study: comparison of theoretical and numerical results

In the following, a gable folded roof shell is proportioned by addressing the simplified method; the case study refers to a plywood structure resisting the roof vertical loads ($p=3.0 kN/m^2$, where $g=q=1.5 KN/m^2$). The geometry of the gable roof, as well as the material mechanical characteristics, are those illustrated in Table 1. The folded roof shell behavior predicted by the simplified method is then compared to the numerical results of linear finite element analyses in terms of ridge and eave chord maximum axial forces (F_{11} and F_{13}), shear flow and slip along the horizontal joints between the panels (q and δ_1), and maximum vertical and horizontal displacements (w_{max} and η_{max}) at the folded roof shell mid span.

3.1 Proportioning of the folded roof shell components

With reference to the geometry illustrated in Table 1, the folded roof shell components are proportioned based on the estimate of the maximum chord axial force, panel shear flow and the structure deformation, as predicted by the analytical simplified model.

In the case study, the roof rafters are assumed as hinged along the ridge line, thus the vertical load bearing on the folded roof shell ridge (eq. 1a) and the pitch in-plane load (eq. 2) are, respectively, equal to:

$$f_{1z} = p l_{12} = 3.0 \cdot 5.39 = 16.17 \text{kN/m}$$

$$f_1 = \frac{f_{1z}}{2\text{sen}\alpha} = \frac{16.17 \text{N/m}}{2\text{sen}22} = 21.58 \text{kN/m}$$

The maximum bending moment and shear force are equal to:

$$M = \frac{f_1 L_x^2}{8} = \frac{21.58 \cdot 20.6^2}{8} = 1144 \text{kNm};$$

$$V = \frac{f_1 L_x}{2} = \frac{21.58 \cdot 20.6}{2} = 222 \text{kN}$$

The maximum eave and ridge chord axial force, and the maximum shear flow in the web panel are:

$$F_{13} = \frac{M}{l_{12}} = 212.2 \text{kN}$$

$$F_{11}=2F_{13}=424.4\text{kN}$$

$$q=\frac{V}{l_{12}}=41.18\text{kN/m}$$

Based on the calculated maximum internal forces, the plywood folded roof shell components are designed. The eave and ridge chords cross sections (A_{13} and A_{11}, respectively) and web panel thickness *s* are proportioned as follows:

$$A_{13}=3750\text{mm}^2;\ A_{11}=2A_{13} \qquad \sigma_s=\frac{F_{13}}{A_{13}}=56.7\text{MPa}$$

$$s=27.5\text{mm} \qquad \tau=\frac{q}{s}=1.5\text{MPa}$$

In order to avoid the compressed chord uplift induced by instability, anchorages and screws fixing the chord to the wall and to the wood panels are needed. The maximum anchorage spacing Δx_a depends on the thickness of the chords. The adopted reduced steel stress value $\sigma_s = \chi f_{yd} \cong 100$ MPa yields an instability reduction factor $\chi = 0.35$ (for $f_{yd} = 280\,\text{MPa}$). This reduction factor corresponds to a slenderness approximately equal to $\lambda \cong 120$. The effective length is equal to:

$$l_o = \lambda \frac{t_c}{\sqrt{12}} = \frac{120 \cdot 20}{\sqrt{12}} \cong 0.7\,\text{m}$$

being t_c = 20 mm the thickness of the eaves chord steel plate.

The maximum anchorage spacing Δx_a , yields as follows:

$$\Delta x_a = 2\, l_o = 1.4\,\mathrm{m}$$

The connections between the web panels are made of slender steel nails (d=4mm) with a spacing Δx=50mm. Each nail connection has an elastic stiffness k_n = 2700 N/mm (as proposed in Giuriani and Marini, 2008a), thus the maximum slip of the connection is equal to:

$$s_n = \frac{q\Delta x}{k_n} = 0.76\mathrm{mm}$$

In order to account for the shear deformability of the nail connections between adjacent plywood panels (vertical nail connections, *a* in Fig. 12a), equivalent elastic moduli are assumed as equal to $G_w^* = 510\mathrm{MPa}$ (Eq.18) and $E_w^* = 953$ MPa (Eq.20).

Given the plywood panel arrangement, an additional deflection is expected to follow the relative slips occurring along the horizontal nail connections between the plywood panels at the web panel mid height (the slip is equal to $s_{nb} = 2s_n$ along the alignment *b* in Fig. 12a) and at the interface between the eave and ridge chords with the web panel (the slip is equal to $s_{nc} = s_{nc'} = s_n$ along both the alignment *c* and *c'* in Fig. 12a). It yields:

$$y_{max} = \frac{5}{384}\frac{f_l L_x^4}{E_w J_{id}} + \frac{\chi}{8 G_w A_w} f_l L_x^2 + \frac{4 s_n}{3.2}\frac{L}{H} =$$
$$= 4.3 + 8.5 + 3.6 = 16.4\mathrm{mm}$$

which entails a vertical (w_{max}) and horizontal (η_{max}) displacement equal to:

w_{max}=43.9mm (=1/469 L_x);

η_{max}=17.7mm (=1/1163 L_x).

3.2 Numerical analyses

The static behavior of the case study gable folded roof shell is then compared with the results of some linear elastic finite element analyses performed with Strauss software. In the FE mesh only the roof is modeled; the lateral masonry walls are represented by vertical hinged beam elements, inhibiting any vertical displacement of the roof along the eaves lines, but allowing horizontal transverse displacements and rotations (Fig. 13). The head gables are modeled as in-plane rigid diaphragms, allowing out-of the plane displacements and rotations.

Two different Mesh Types are analyzed (see Giuriani et al., 2002 for further case studies):

- in *MESH A*, all structural elements composing the existing wooden roof and the overlaying folded shell are modeled, and all vertical loads are considered (Fig. 13a). Wooden rafters and ridge beam, as well as steel eave and ridge chords are modeled by means of beam elements, whereas pitch web panels are modeled as plate elements. Rafter to pitch diaphragm stud connections are modeled as one-dimensional linear elastic springs. The deformability of the nailed shear connections between the pitch web panels was considered by introducing along every connection special plate elements having a reduced equivalent elastic $E^*_{w,A}$ and shear moduli $G^*_{w,A}$. Geometric and mechanical characteristics of each element are those illustrated in Table 1.

- In *MESH B* only the folded roof shell was modeled (Fig. 13b), as the folded shell folded shell was assumed to be independent of the frame behavior of the wooden rafters. Accordingly, only the ridge vertical load per unit length f_{lz} was considered (Fig. 7a). In *MESH B* the folded roof diaphragms were modeled by means plate elements as in *MESH A*. Geometric and mechanical characteristics of each element are those illustrated in Table 1.

The preliminary analyses performed on *MESH A* and *B1* (see Tab. 2) compared well in terms of chord axial force, shear flow and displacements distribution. Further parametric analyses were performed on *MESH B1* only. Further numerical case studies are presented in Giuriani et al., 2002.

3.3 Comparison of numeric and analytical results

In Figures 14a the chord axial forces are plotted for varying the eave and ridge chord cross section. In the analytical model, the assumed chord and panel structural behavior, results in the prediction of constant chord axial forces. In the numerical model, the eave and ridge chord axial forces asymptotically approach the analytical solution for increasing the chord cross section. In the case of smaller chord cross sections, the contribution of the web panel in resisting the bending moment cannot be neglected and the analytical solution appreciably overestimate the actual axial forces. Noteworthy, as expected, the analytical solution always represents a conservative prediction of the chord axial force and can be conveniently adopted for the folded roof shell component proportioning.

Figure 14b shows the maximum structure deflection along the ridge line w_{max} and the maximum slide at the eaves η_{max} for varying chord cross section areas. Theoretical and numerical results compare very well. The structural deformability significantly increases (w_{max} and η_{max} nearly double) for decreasing the chord cross sections; interestingly, however, the deflection to span ratio is always very low, confirming that the proposed folded roof shell is quite stiff and displacements are rarely a concern.

4. Retrofit of ancient buildings

4.1 San Pietro in Berbenno, Italy (XVI century)

Figure 15a shows an internal view of the main nave and side aisles of San Pietro church in Berbenno, a small town located in the Alps, Italy. The roof is composed of a simple framing with ridge beams simply supported on the transverse arches, and roof rafters simply supported on the ridge beams, the nave arcade and the longitudinal walls (Figure 15b). The roof was strengthened in 1995 in order to upgrade the capacity against severe vertical loads, induced by the heavy roof covering made of stone slabs and by the snow (total load 5KN/m^2). To this end, a plywood folded shell overlaying the existing wooden plank was conceived and additional stays were introduced in order to upgrade the folded shell shear resistance (Figure 15c).

4.2 Nun monastery, Desenzano, Italy (XVIII century)

Figures 16 show some internal views of the gym hall of a school in Desenzano, formerly a nun monastery. During the restoration works (carried out in 1990), existing wooden truss-works of

no historical value were removed and the attic floor was cleared from partitioning walls. A thin concrete folded shell was built on top of the existing wooden roof to resist the wood rafter lateral thrusts and to avoid significant displacements along the eave edges upon removal of the wooden truss-works.

The gym hall plan is about 25.5x10.3mq. The roof pitch angle is 24°. The roof structure is composed wooden rafters (cross section 140x200 mm), spaced 500 mm apart, covered by 25 mm pine wood planks. The thin reinforced concrete slab (50 mm thick, with two 5 mm/200x200mm steel meshes) is connected to the wooden roof by means of steel studs (d= 16 mm). Eaves and ridge chords, as well as hip diagonal beams are made of reinforced concrete, encased in wooden boards.

The structure displacements were monitored for more than one year after construction (Fig. 16b). The maximum displacement was recorded at the roof mid span and was equal to 4 mm and no significant deferred deflection due to creep was recorded. No crack pattern developed on the structures and no appreciable out of plumb was surveyed on the perimeter masonry columns. The surveyed displacements matched with the theoretical predictions, and proved the efficient confinement of the rafter lateral thrust attained with the roof folded diaphragm.

5. Final remarks

Historic masonry buildings often require the stiffening and strengthening of the existing wooden roof with respect to both the vertical and horizontal loads, also to comply with the current Standard requirements concerning the snow loads or the seismic action. In this paper a technique

is proposed for the retrofit of existing wooden roofs against vertical loads. With some minor adaptations, the technique can be as well adopted for the seismic retrofit of existing buildings. The solution is based on the construction of a thin folded shell overlaying the existing roof rafters and planks. The folded shell transfers the main part of the vertical load on the roof to the head gable walls thanks to the organization of each pitch plane to behave like a deep beam in its own plan, simply supported on the head gable walls. The folded shell of the roof allows removing intermediate supports of the ridge beams, such as bulky truss-works or columns, necessary in some restoration project when the conceived new use of the attic floor might entail the clearing of the attic volume. Secondarily, it makes the roof stiffer against vertical loads, implying a reduced deflection of existing ridge beams and the related lateral thrust of the roof rafters on the peripheral walls, thus preventing the latter from excessive out-of-plumb.

The paper elaborates a rational conceptual design of the folded roof shell defining the role of each component, namely chords, web panels, head gable walls, rafters and their mutual connections. Focus is made on the importance of the construction details for the effectiveness of the structural solution and on the equilibrium equations necessary for the rational proportioning of each element. A simplified analytical method is proposed, which allows identifying the static role of each component of the folded roof shell and can be usefully addressed for the structure proportioning and design. The simplified method can be as well adopted to verify the results obtained with more sophisticated analytical tools or numerical analyses.

The efficiency of the proposed solution is proved by the results of post-intervention monitoring of the deformations in some real applications. Moreover, an example of folded roof shell

proportioning and calculation according to the proposed simplified formulation is compared with the results of numerical modeling. Different level of modeling refinement were used that showed the reliability of the assumptions taken in the simplified analytical model.

The model provides an estimate of the structural deformability, also accounting for the effect of the nailed connections, which significantly reduce the overall stiffness of the plywood overlay. The deflection of the folded shell subjected to the vertical loads is quantified in terms of roof ridge vertical displacement and eave lateral horizontal displacement, the latter being particularly important for the control of the peripheral wall out-of-plane deformation.

Noteworthy, the folded shell is typically sufficiently rigid so that deformability problems are not of any concern. Conversely, the correct proportioning and assemblage of each component and connection is of primary importance in order to ensure the efficient global behavior.

The technology is rather simple but it requires very attentive assemblage of each component, mindful care of the structure detailing, and may necessitate special man labor and continuous supervision during construction.

In this paper, among all possible technics, emphasis was given to the wooden lightweight folded diaphragm, which can be obtained by superimposing plywood panels to the existing wooden roofs. When necessary the folded shell can be strengthened with an overlaying additional stay structure made of thin steel flanges.

The proposed technique meets the requirements of the modern restoration principles: it is mainly reversible and does not impair the building integrity.

Acknowledgements

This work was developed within the research project DPC-RELUIS 2013–2015, Research line n. 1: *Masonry Structure*. RELUIS financial contributions is gratefully acknowledged.

References

Benedetti, D. 1981. Riparazione e consolidamento degli edifici in muratura. In AA.VV. *Costruzioni in zona sismica*, Cap. 11. Milano, Italy: Edizioni Masson.

Bruhn, E. F. 1973. *Analysis and design of flight vehicle structures*. Indianapolis, IN: Jacobs Publishing Inc.

Eurocode 5.UNI EN 1995:2005: Design of timber structures - Part 1-1: General - Common rules and rules for buildings.

Felicetti, R., Gattesco, N., Giuriani, E. 1997. Local phenomena around a steel dowel embedded in a stone masonry wall. *Materials and Structures.* 30, 238–246

Gattesco, N., Del Piccolo, G. 1998. Shear transfer between concrete members and stone masonry wall through driver dowels. *European Earthquake Engineering*, 1.

Gelfi, P., Ronca, P. 1993. Il consolidamento dei solai in legno: studio sperimentale sui connettori tra trave in legno e cappa in calcestruzzo armato. *L'Edilizia*, n. 5, 41-50.

Gelfi P., Giuriani E., Marini A. 2002. Stud shear connection design for composite concrete slab and wood beams. ASCE Journal of Structural Engineering. Vol. 128, n.12, pages 1544-1550. ISSN 0733-9445.

Gelfi, P., Giuriani, E. 2003. Influence of Slab-Beam Slip on the Deflection of Composite Beams. International Journal for Restoration of Buildings, Aedificatio Verlag, Freiburg, Vol. 9, No 5, pag. 475-490, ISSN 0947-4498

Giuriani, E., Frangipane, A. 1993. Wood-to-concrete composite section for stiffening of ancient wooden beam floors. Atti del 1° *Workshop Italiano sulle Strutture Composte*, Trento, Italy, June 17–18, 1993. Trento, Italy: Universita` degli studi di Trento. In Italian.

Giuriani, E., 1997. *Recupero e consolidamento delle strutture*. In: Mezzanotte, G., Belotti, G., Giuriani, E., Piemonte, C.. Percorsi del restauro in San Faustino a Brescia. Ed. Il Polifilo. p.153-180. Milano.

Giuriani, E., Guilarte, F., Marini, A., Tonioli, A. 2002. Comportamento sismico delle coperture in legno. *Technical Report*, 19-2002, Brescia, Italy: Universita` degli Studi di Brescia, Dipartimento di Ingegneria Civile. (In Italian) @researchgate.net

Giuriani, E., Marini, A. 2008a. Wooden roof box structure for the anti-seismic strengthening of historic buildings. *Journal of Architectural Heritage: Conservation, Analysis and Restoration*. ISSN 1558-3058 Vol.2(3) Pag. 226-246.

Giuriani E., Marini, A. 2008b. Experiences from the Northern Italy 2004 earthquake: vulnerability assessment and strengthening of historic churches. Invited paper. *VI International Conference on Structural Analysis of Historical Constructions SAHC 2008*. 2-4 July, Bath, England. pag. 13-24. Ed. Taylor and Francis, London, UK. ISBN 978-0-415-46872-5**.**

Giuriani, E. 2012. Consolidamento degli edifici Storici. UTET.

Giuriani, E., Marchina, E., Cominelli, S., Molinari, A. 2014. Indagine sperimentale su diaframmi di piano antisismici realizzati con doppio assito. Technical Report, 7-2014. Department of Civil Engineering, Architecture, Land, Environment and Matemathics of the University of Brescia. (In Italian) @researchgate.net

Griffith, M. C., Magenes, G., Melis, G., Picchi, L. 2003. Evaluation of out-of-plane stability of unreinforced masonry walls subjected to seismic excitation. *Journal of Earthquake Engineering* 7(special issue 1): 141–169.

Humbert, J., Boudaud, C., Baroth, J., Hameury, S., Daudeville, L. 2014. Joints and wood shear walls modelling I: Constitutive law, experimental tests and FE model under quasi-static loading, Engineering Structures, Volume 65, 15 April 2014, Pages 52-61, ISSN 0141-0296, http://dx.doi.org/10.1016/j.engstruct.2014.01.047.

Timoshenko, S.P., Woinowsky-Krieger, S. 1989. Theory of plates and shells. New York: McGraw-Hill.

Meda, A., Riva, P. 2001. Strengthening of wooden floors with high performance concrete slabs. *International Journal for Restoration of Buildings and Monuments* 7(6):621–640.

Peralta, D. F., Bracci, J. M., Hueste, M. B. D., 2004. Seismic behaviour of wood diaphragms in pre-1950s un- reinforced masonry buildings. Journal of Structural Engineering, 130(12): 2040-2050.

Piazza, M., Turrini, G. 1983. Il recupero statico dei solai in legno. Recuperare (7): 396–407. In Italian.

Figure 1: Examples of folded roof diaphragms adopted for the retrofit against vertical loads of some monumental buildings in Brescia, Italy: (a) University head quarter (exterior perspective view of the building, internal view of the existing wooden joists and top view of the strengthening plywood folded roof diaphragms with edge steel plate chords , overlaying the existing wooden roof, 2001); (b) Head administrative office of the University hosted in the former San Faustino Monastery XV century (exterior perspective views of the building, and top view of the plywood folded roof diaphragms further strengthened with additional strengthening steel stays, 1990; (Giuriani 1997).

Figure 2: Folded roof shell components.

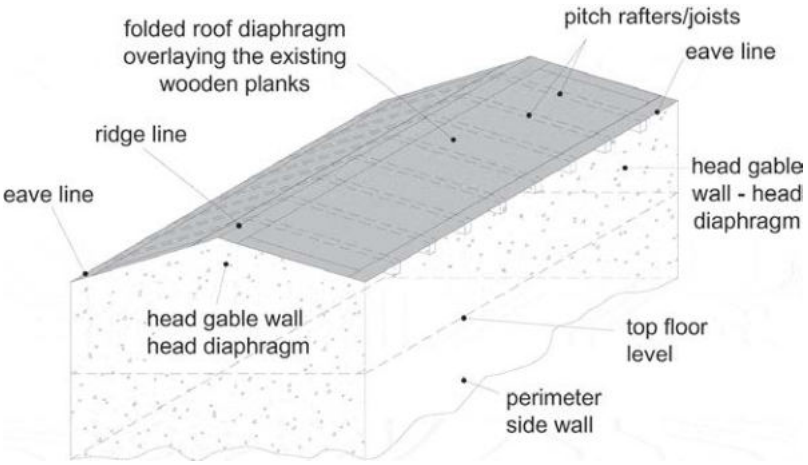

Figure 3: Gable roof: structural elements for the wooden roof strengthening.

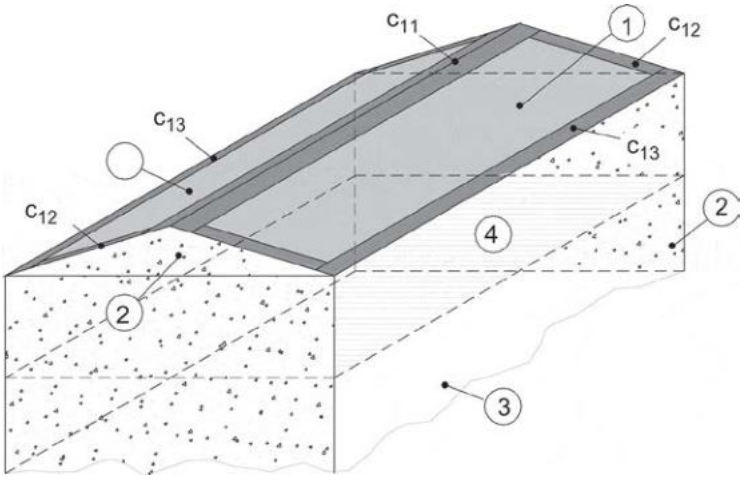

Figure 4: (a) Damage caused by the wooden joist lateral thrust applied to the wall crowning masonries; (b) the larger the deformability of the ridge beam, the larger the lateral thrust applied to the crowning masonry walls.

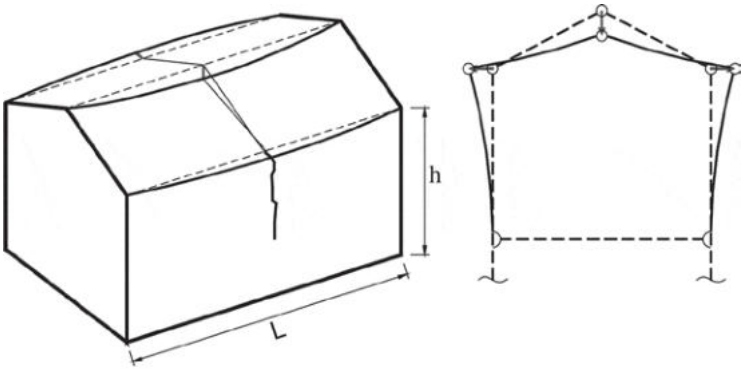

(a) (b)

Figure 5: Wooden floor in plane shear strengthening by means of overlaying (a) plywood panels; (b) inclined overlaying wooden planks; (c) new orthogonal wooden planks; (d) thin concrete slab; (e) thin high performance concrete slab.

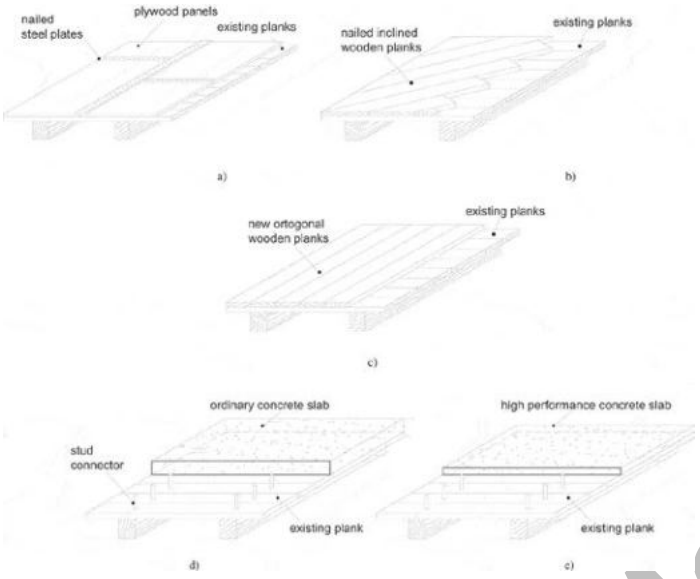

Figure 6: Frame action and folded roof shell undergoing vertical ridge loads.

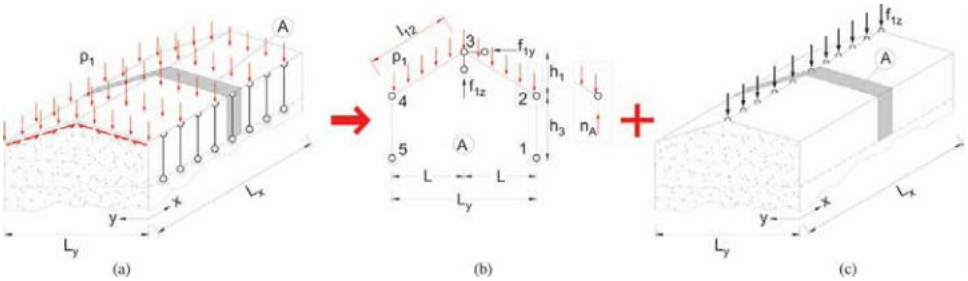

Figure 7: a) Pitch diaphragm loading condition and internal action distribution; b) and c) details of the rafter to web panel connection (structural detail of node 3 in Figure 6b); d) Stud connectors transferring the rafter axial force *Nr* to the diaphragms, as load per unit length f_1;V_d is the shear load in the connection; e) detail of the connection to the perimeter walls (node 4 in Figure 6b; this connection is mandatory in seismic conditions only, but is suggested also in the case of retrofit against vertical loads)

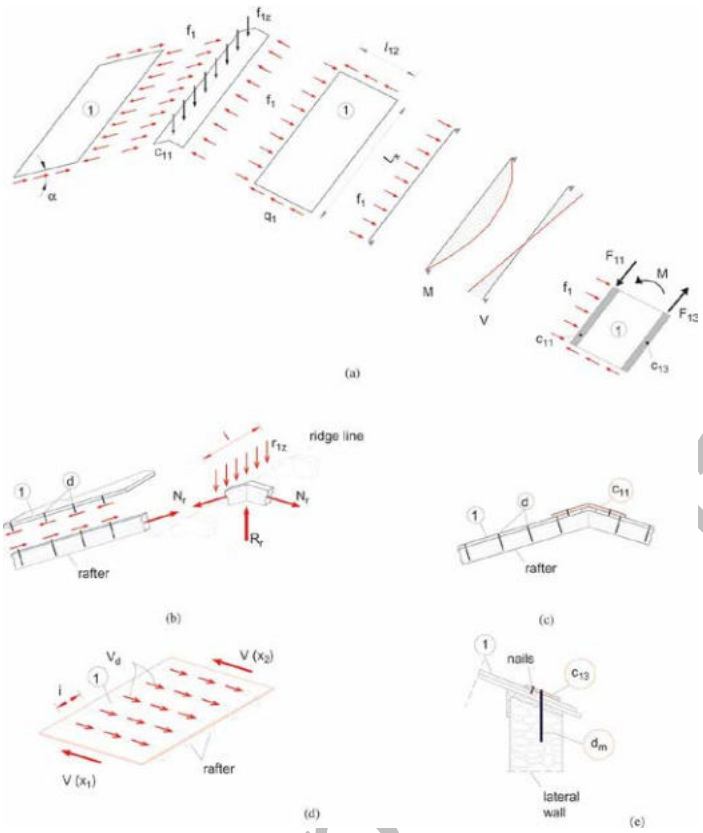

Figure 8: Alternative solutions to engineer the head wall with appropriate devices in order to resist to the shear flow q_1

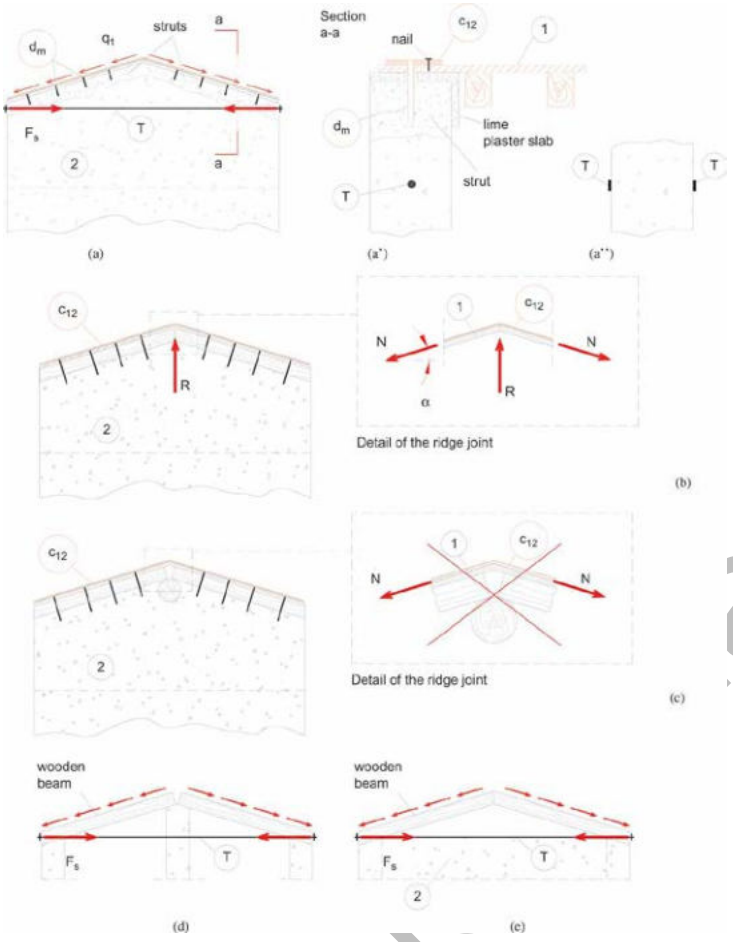

Figure 9: Supplementary stay structure enhancing the shear resistance of the roof folded diaphragm.

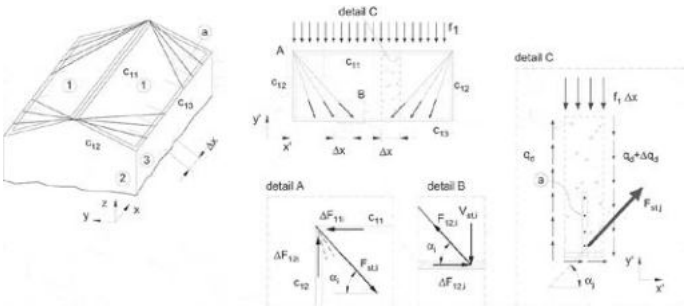

Figure 10: Shear force demand vs shear resistance.

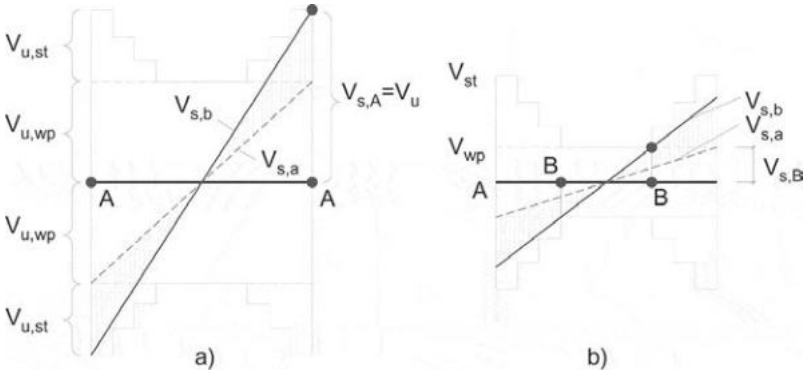

Figure 11: Cinematic mechanism the roof pitches. Details A and B: closer view of the deformation of the Folded roof shell at the eave and ridge line.

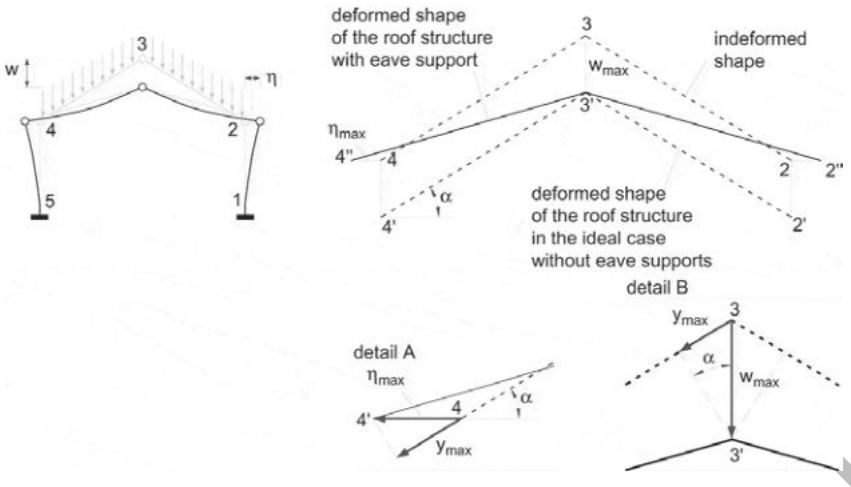

Figure 12: (a) Arrangement of the plywood panels; (b) simplified evaluation of the modified equivalent shear modulus; and (c) the equivalent Young modulus (Giuriani and Marini, 2008a); d) Details of the pitch diaphragm at the supports, showing the in-plane incremental deflection $\Delta\varphi$ induced by the slip s_{ni} occurring along the horizontal alignments b, c and c' (alignments shown in Figure 12a).

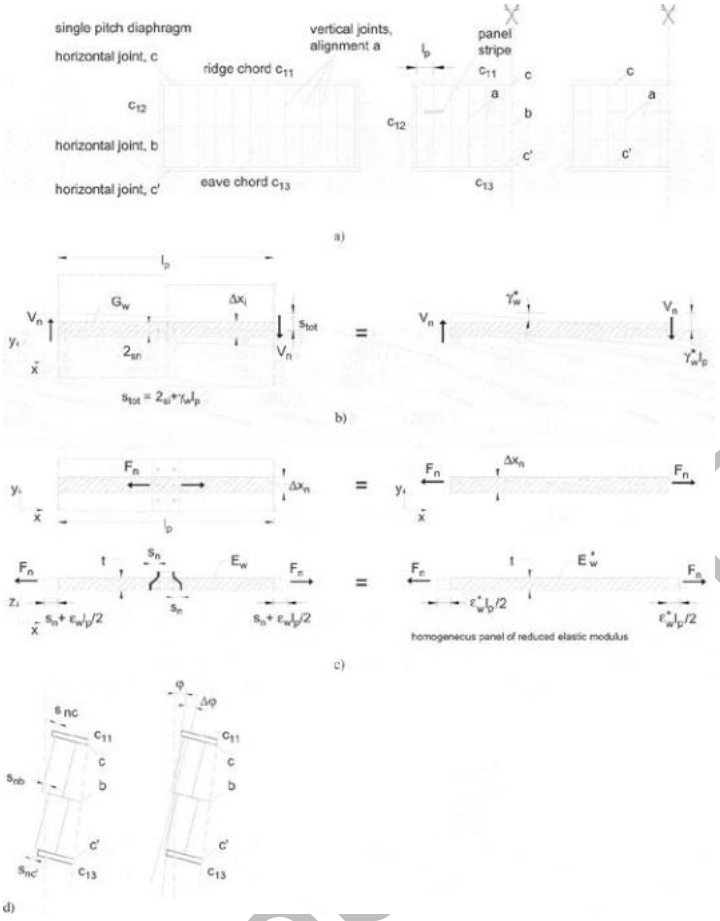

Figure 13: Numeric Models: (a) *MESH A* – all element composing the existing roof and the complementing folded shell are modelled. The static model of each structural component is described in the figure. The diaphragm stiffness reduction caused by the nailed connections is modelled by introducing thin strips of plate elements having reduced mechanical properties along the interfaces of adjoining plywood panels (grey elements of the mesh). The load per square meter p is applied along the ridge line.(b) *MESH B* – same as for *MESH A*, except that in this case the sole pitch diaphragm is modelled, whereas the rafters are removed from the mesh; and the load per unit length f_{1z} is applied along the ridge line.

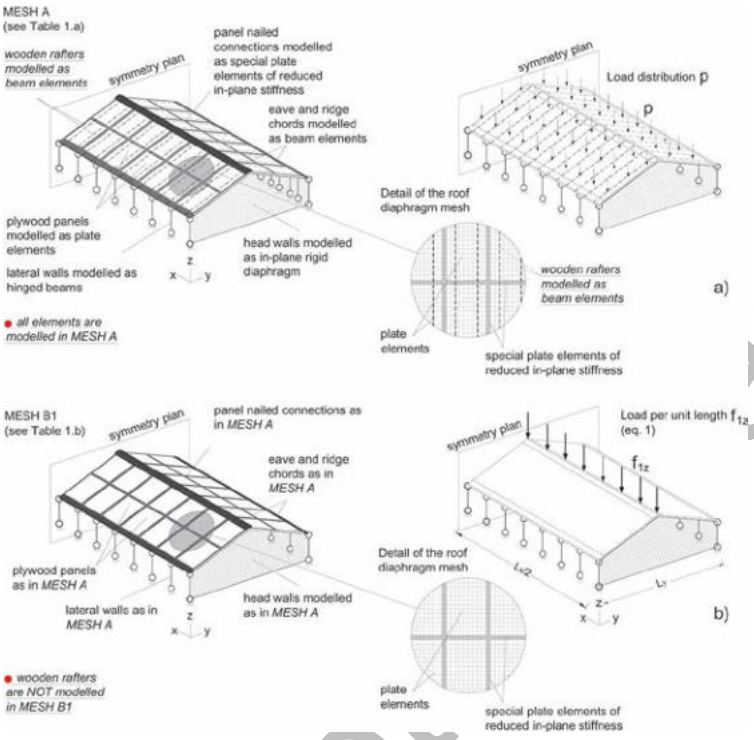

Figure 14: a) η_{max}, w_{max}, and b) F_{11} and F_{13} for varying the eave and chord cross sections

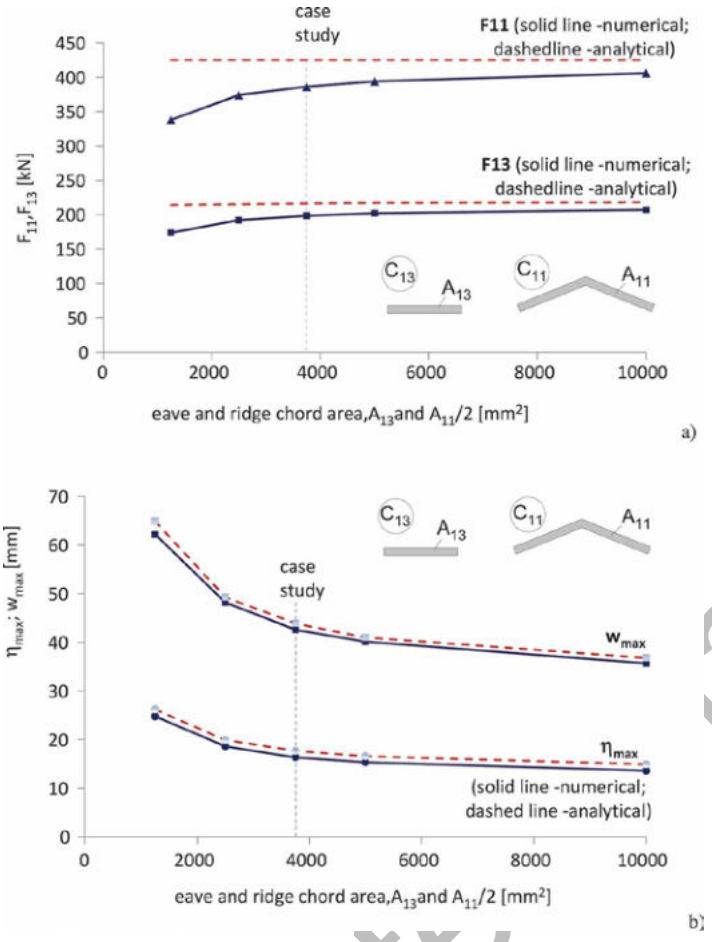

Figure 15: San Pietro in Berbenno (XVI century), Sondrio, Italy: (a) view of the church; (b) internal view of the main nave and the lateral aisles; (c) view of the plywood folded roof diaphragm, strengthened with additional steel stays; (d) load test carried out upon completion of the structural intervention.

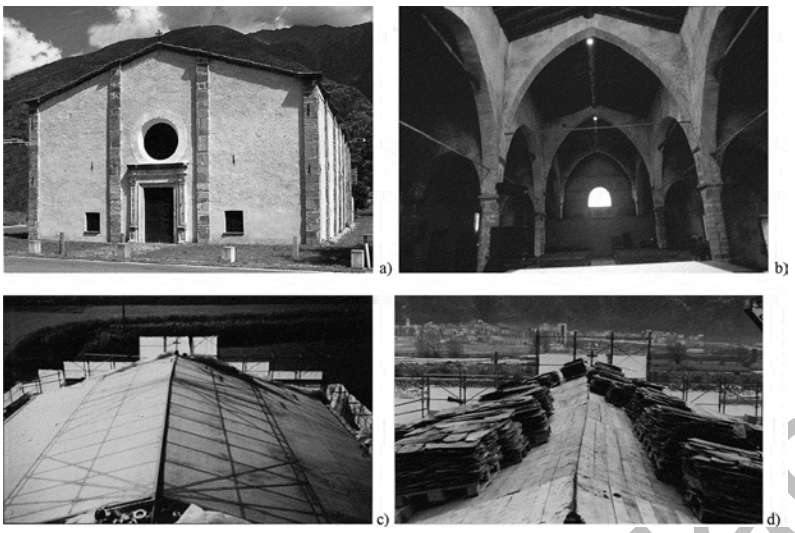

Figure 16: Nun Monastery, Desenzano, Brescia, Italy (XVIII century): (a) internal view of the hipped wooden roof, strengthened with a collaborating thin concrete slab (50mm); (b) monitoring of the maximum deflection over time (note the aluminum profile bridging the lateral walls); (c) load test carried out upon completion of the structural intervention.

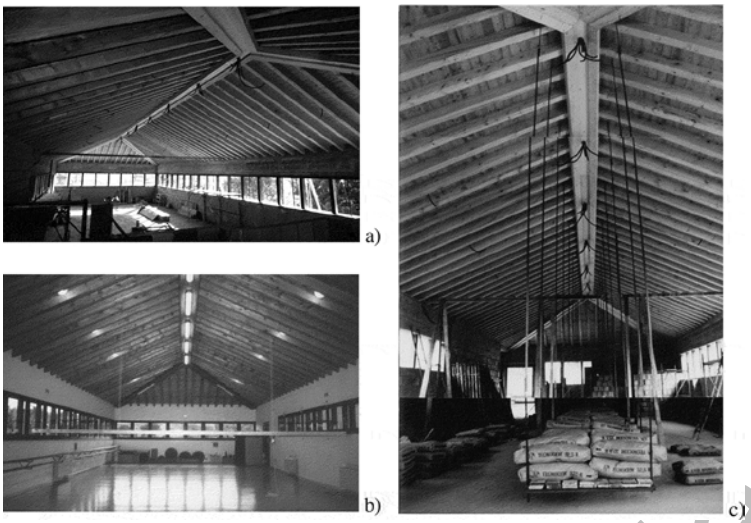

Table 1. Geometry of the gable roof, and material mechanical characteristics.

Roof geometry (Fig. 6)	L_x = 20.6 m; L_y = 10m; α = 22°; l_{12} = 5.39 m
Folded roof shell components	*Plywood web panel* (Fig. 12): Single panel geometry and mechanical properties: l_p = 1200 mm, t_p = 27.5 mm E_w = 5000 MPa; $_{Gw}$ = 4000 MPa *Web Panel nailed connection*: d = 4mm, Δx_i = 50mm k_n = 2700 N/mm (Giuriani and Marini, 2008a) *Steel Eave and ridge chord*: A_{11}= A_{13}=3750mm^2 E_S = 210000 MPa
a) MESH A:	*Plywood web panel*: Ew = 5000 MPa; Gw = 4000 MPa

	Reduced elastic modulus for elastic plate elements modelling the nail connections between the panels (a and b in Fig. 12a): In order to correctly represent the target shear modulus $G^{*}_{w,a}$ = 95.8 MPa (obtained by setting l p=100 mm in eq.18), Young's and Poisson's moduli were set equal to $E^{**}_{w,a}$ = 207 MPa; ν=0.1 in the model *Reduced elastic modulus for elements modelling the connection between the panels and the chords* (c and c' in Fig. 12a): Focus is paid to correctly represent the sole target shear modulus, which is obtained by setting lp=100 mm in eq.18 and by correcting eq. 18 to account for the single line of nailed connections. It yields: $G^{*}_{w,c} = \frac{k_n l_p}{A_{wn} + \frac{k_n l_p}{G_w}} = 187.2 \text{MPa}$ Thus, in the model $E^{**}_{w,c}$ = 469.8 MPa; ν=0.1 *Roof rafters*: b_w=120mm, h_w=240mm, i=600mm; E_w = 10000 MPa *Ridge beam*:

	b_w=240mm, h_w=280mm; E_w = 10000 MPa *Stud connections* (4 studs per rafter) *between roof rafters and plywood web panels*: d = 20mm; K = 8700N/mm
b) MESH B	Same as in *MESH A*, except that the wooden rafters and ridge beams are removed from the mesh.

Table 2. Comparison of analytical estimates and numerical results.

	F_{11} [kN]	F_{13} [kN]	τ_{med} [MPa]	s_{nb} [mm]	w_{max} [mm]	w_{max} / L [-]	η_{max} [mm]	η_{max} /L [-]
MESH A	386	197	1.41	1.1	41.2	1/500	16.5	1/1248
MESH B	386	198	1.45	1.1	42.6	1/483	16.3	1/1263
ANALYTICAL	424	212	1.5	0.76x2	43.9	1/469	17.7	1/1163